Journal of Materials Chemistry C

Accepted Manuscript

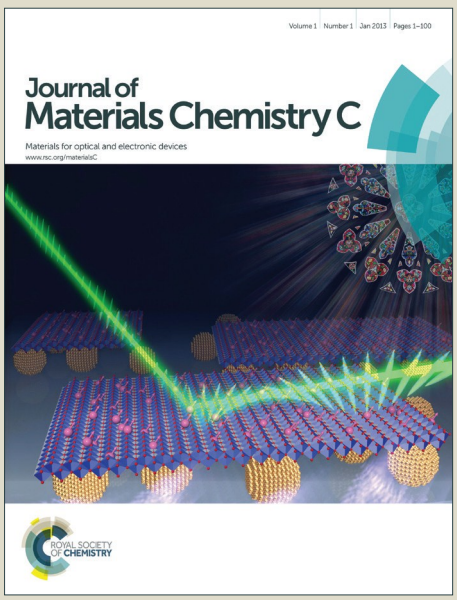

ROYAL SOCIETY OF CHEMISTRY

www.rsc.org/materialsC

J Mater Chem C

ARTICLE

Size and morphology effects on fluorescence properties of π-conjugated poly(*p*-phenylene) polyelectrolyte nanoparticles synthesized via polyion association

Received 00th January 20xx,

Accepted 00th January 20xx

DOI: 10.1039/x0xx00000x

www.rsc.org/

Hiroshi Yao*[a] and Chiaki Fukui[a]

A facile method is developed to synthesize π-conjugated polymer nanoparticles of propoxy-sulfonated poly(*p*-phenylene) polyelectrolyte (PPP-SO). The synthesis is based on nano-agglomeration via polyion association in poor solvent (termed as *NAPA* approach), which involves polyion complex formation between the anionic PPP-SO and cationic poly(diallyldimethylammonium) (PDDA) and subsequent nano-globulization. Size tuning is successful by varying the net charge ratio between PDDA and PPP-SO. Salient features of the present PPP nanoparticle system include a dual emission property; in particular, small nanoparticles exhibit a prominent green-site emission (λ_{em} ≥ ~500 nm). Since a small particle has a large surface-to-volume ratio, the green-site fluorescence is reasonably associated with the surface (or interfacial) region on the ion-based polymer nanoparticles. On the basis of fluorescence anisotropy for the PPP nanoparticles, the green-site emission can be due both to the energy transfer (or exciton migration) to a structural trap-site on the polymer backbones and exclusive excitation of the chromophoric segments having a long effective conjugation length, where the contribution of the latter mechanism is significant when the size becomes small.

Introduction

Fluorescent nanoparticles have been demonstrated in a wide range of applications such as optoelectronic devices, live cell imaging, and/or intracellular dynamics.[1] Among such nanoparticles, π-conjugated polymer nanoparticles possessing high absorption coefficients and fluorescence efficiencies are one of the promising candidates, so there is growing interest in their study.[2–5] In particular, their easy synthesis, less toxicity and more biocompatibility compared to common inorganic nanoparticles further make these nanomaterials highly attractive.[3] So far, typical π-conjugated polymer nanoparticles have been synthesized by a miniemulsion or reprecipitation method.[3] In the miniemulsion technique, a polymer is normally dissolved in a water-immiscible organic solvent and the resulting solution is injected into an aqueous solution including some surfactants.[6,7] In this method, the particle size can be changed from several tens to hundreds of nanometers depending on the concentration of the polymer solution. The reprecipitation method, on the other hand, consists of a hydrophobic conjugated polymer dissolved in a good (organic) solvent that can be poured into a poor solvent (typically water), which is miscible with the good (organic) solvent.[8] The resulting mixture is stirred vigorously to fold into nearly spherical shapes to minimize the contact area (nanoparticle formation). In both methods, polymers are usually limited to highly hydrophobic conjugated polymers carrying almost no functional groups to be further modified.[3]

Meanwhile, on the basis of our successful approach in preparing ion-based organic nanoparticles composed of small (or low molecular weight) molecules,[9] a new route for the synthesis of ionic polymer (or polyelectrolyte) nanoparticles has been developed.[10] This method utilizes the phenomenon of *n*ano-*a*gglomeration via *p*olyion *a*ssociation (termed as *NAPA* approach), which includes polyion complex formation and subsequent globulization to fabricate nanoarchitectures in water-miscible liquid.[10] We then found that, in contrast to the dispersion of nanoparticles of non-ionic, hydrophobic π-conjugated polymers, which can be mostly prepared by the simple reprecipitation method,[8] the *NAPA* approach prevents further bending or kinking of the conjugated polymer backbone upon the ion-pair nanoparticle formation.

[a] *Graduate School of Material Science, University of Hyogo, 3-2-1 Koto, Kamigori-cho, Ako-gun, Hyogo 678-1297, Japan. Fax: 81-791-58-0161; E-mail: yao@sci.u-hyogo.ac.jp.*

† Article for themed issue on "Shape-Responsive Fluorophores".

Electronic Supplementary Information (ESI) available: [Emission spectrum of the PPP-SO/PDDA film prepared by a drop cast of the 2-propanol solution]. See DOI: 10.1039/b000000x/

In the present study, synthesis and spectroscopic properties of π-conjugated polyelectrolyte nanoparticles are explored to achieve emission color tuning as a function of their particle size, since there is still interest in the development of conjugated polymer nanoparticles with red-shifted or dual emission spectra.[11] A water-soluble poly(*p*-phenylene) (PPP) derivative is chosen for this study because PPP analogues are especially important mostly due to their high conductivity when doped with either *n*-type or *p*-type dopants,[12] the active constituents of blue light emitting diodes,[13] and high thermal and oxidative stability,[14] despite a lack of general processability when they are unsubstituted.[15] Conjugated polymer (polyelectrolyte) nanoparticles of a sulfonate-substituted PPP derivative (PPP-SO) are successfully synthesized in the presence of cationic polyelectrolytes on the basis of the NAPA approach. We then examine their photophysical properties including excitation energy transport (or exciton migration) using fluorescence anisotropy technique, and find that a relatively increased efficiency of green-site emission is observed particularly for the nanoparticles, bringing about a dual emission behavior. In addition, the origin of the green-site emission is discussed in terms both of a structural trap-site and effective conjugation length of the polymer.

Experimental

Materials

The anionic π-conjugated polyelectrolyte, poly(2,5-bis(3-sulfonatopropoxy)-1,4-phenylene-*alt*-1,4-phenylene) sodium salt, (abbreviated here as PPP-SO, chemical structure is shown in Fig. 1), one of a larger class of poly(*p*-phenylene) (PPP) derivatives, was received from Aldrich and used without further purification. The precise molecular weight of PPP-SO has not been disclosed, but it will be deduced from the fact that absorption maximum (λ_{max}) values of π-π* transition can be approximately used as a standard to predict the *minimum degree* of polymerization (or molecular weight) for the PPP-SO polymer.[16] For the PPP-SO polyelectrolyte used in this study, the λ_{max} value (~339 nm) of π-π* absorption in water was almost the same with that reported by Reynolds and co-workers,[16] suggesting the molecular weight of $M_w = 1\sim2 \times 10^4$ (or 40~80 phenylene rings per chain).§ Positively charged polycation poly(diallyldimethylammonium) chloride, abbreviated as PDDA; average $M_w = 1\sim2 \times 10^5$, was chosen as an ion-associable counterion (see also the chemical structure in Fig. 1). 2-Propanol (GR grade) was obtained from Wako Pure Chemicals. Pure water was obtained by a water-distillation supplier (Advantec GS-200).

Synthesis

2-Propanolic PPP-SO/PDDA mixtures create "PPP nanoparticles". The polymer nanoparticles of PPP-SO were prepared by means of our newly developed approach based on polyion association (NAPA approach).[10] Typically, rapid addition of a mixture containing PPP-SO (aqueous, 0.01 wt%, 0.5 mL) and PDDA (aqueous, 0.02 wt%, 0.17 mL) into ultrasonicated 2-propanol (5.0 mL) produced almost transparent nanoparticle suspension. In the synthesis, the ratio of ionic equivalents (or net charge ratio; ρ = [PDDA]/(2 × [PPP-SO]) in monomer units, was changed from 1 to 4. The content of water kept unchanged. The resulting suspension was stored overnight at room temperature and examined by spectroscopy and microscopy. Note that the spectroscopic properties are predominated by the chromophoric PPP-SO polyelectrolyte, so we hereafter call the samples "PPP nanoparticles".

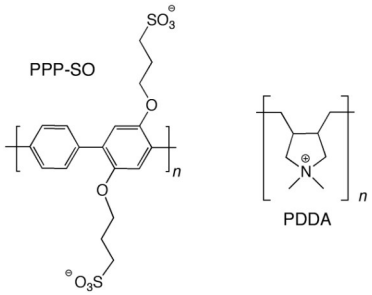

Fig. 1. Chemical structures of PPP-SO (sodium salt) and PDDA (chloride).

Control experiments. For comparison, we prepared a series of reference samples; (i) addition of pristine PPP-SO with Na^+ countercations into 2-propanol (or water) gave the reference solution sample; (ii) mixing of aqueous PPP-SO and PDDA eventually gave deformable "soft-agglomerates" in water. The ρ value was also controlled. Additionally, (iii) "PPP-SO bulk film" was prepared by a drop-cast from aqueous solution of pristine PPP-SO onto a quartz plate. (iv) "PPP-SO/PDDA film" was also prepared in a similar manner to that of the PPP-SO film, but by a drop-cast from PPP-SO/PDDA mixtures in water or in 2-propanol.

Instrumentation

Morphology and/or size of the polymer nanoparticles were examined with a Hitachi S-4800 scanning transmission electron microscope (STEM). UV-vis absorption spectra were recorded on a Hitachi U-4100 spectrophotometer. Fluorescence spectra were obtained with a Hitachi F-4500 spectrofluorometer. For the measurements, all samples were excited at 360 nm. Fluorescence quantum yields (Φ_f) were estimated by comparing the emission spectra of pristine PPP-SO in water with the quantum yield of Φ_f = 0.55 reported by Reynolds and coworkers.[16] We set the absorbance of ~360 nm at ~0.1 and calculated Φ_f values with corrections for the absorbances and the difference in the refractive indices of the solvents (1.333 for water and 1.375 for 2-propanol). Steady-state, wavelength-dependent fluorescence anisotropy (FA) is given

$$FA = \frac{I_{VV} - G \cdot I_{VH}}{I_{VV} + G \cdot 2I_{VH}}$$

where I_{VV} and I_{VH} are the intensities measured with vertically polarized excitation, as indicated by the first subscript, and detected through vertically or horizontally oriented emission polarizers, respectively, as indicated by the second subscript. The *G*-factor $G = I_{HV}/I_{HH}$, which is measured using horizontally polarized excitation, corrects for instrument polarization bias. To set the excitation polarization, Glan-Taylor polarizing prism was used.

Computations

We made calculations for a simple structural model of electrically neutral ion-pair complex of eight cationic 3-ethyl-1,1,4-trimethylpyrrolidinium (a monomer unit of PDDA) and two anionic dimer units of 2,5-bis(3-sulfonatopropoxy)-1,4-phenylene-*alt*-1,4-phenylene to examine how the countercations in the vicinity of anionic PPP influence its geometry and interchain interactions. The ground-state geometry optimizations of the related model complexes were carried out with the Gaussian 09 program at the semi-empirical PM6 level.[17]

Results and discussion

Spectroscopic properties of pristine PPP-SO or PPP-SO/PDDA mixtures in water or 2-propanol

It is known that charged polymers (or polyelectrolytes) can form complexes with oppositely charged polymers, and the produced polyion complex may have a very different geometrical conformation from the free (liberated) charged polymer.[18–20] We then examine whether combination of π-conjugated anionic PPP-SO with oppositely charged PDDA can make the solid-state nanoparticles or not, thereby tune its optical properties.

Fig. 2a shows absorption spectra of pristine PPP-SO in aqueous solution in the absence/presence of PDDA, and Fig. 2b is those in 2-propanol in the absence/presence of PDDA. In pure PPP-SO (no PDDA), the absorption properties were solvent-dependent (solvent effect); that is, the peak position red-shifted as the solvent polarity decreased from water (λ_{max} = 339 nm) to 2-propanol (λ_{max} = 353 nm). The observed peaks are attributed to the lowest π-π* transition that can be derived from benzene excitations polarized with polymer long-axis.[16] On the other hand, the addition of PDDA (ρ = 1) caused a red shift of the absorption peak in both solvents, and their λ_{max} values became almost identical with each other (λ_{max} = 361–362 nm). This feature suggests the existence of strong electrostatic interactions between the anionic PPP-SO and cationic PDDA (that is, polyion complex formation), and the effective conjugation length and degree of structural order along the backbone of PPP-SO are independent on the solvent. It is known that an increased torsional angle between adjacent phenyl rings results in a blue shift in the lowest π-π* transition,[21] so the screening of negative charges existed on alternate rings by positively charged PDDA would lead to a lower energy conformation with smaller torsional angles.[21] The complexation between the cationic/anionic polyelectrolytes can also be driven by favorable entropy changes resulting from release of interfacial water molecules,[18] so such interactions would serve to inhibit the folding of the polymer, reducing the conformational disorder in the π-conjugated backbone.

The more striking spectroscopic feature is the difference in their emission spectra. The emission spectra of PPP-SO or PPP-SO/PDDA mixtures in water and in 2-propanol are shown in Figs. 2c and 2d, respectively. The emission intensity of pristine PPP-SO was rather strong in both solvents, but addition of PDDA caused a significant decrease in the emission intensity. Note that the emission peak had the same position with each other. The decrease in the fluorescence efficiency can be explained by intrachain and/or interchain quenching (also including concentration quenching),[22,23] which should be caused by incorporation of PDDA between adjacent PPP-SO polymer backbones. Interestingly, the appearance of a new emission band (green-site emission; ≥ ~500 nm) is obvious for the PPP-SO/PDDA mixture in 2-propanol (see the inset in Fig. 2c), suggesting formation of a low-energy emissive center (regarded here as a low-energy (low-lying) defect or trap-site including molecular aggregation and/or structural disorder), or existence of facile conformational relaxation by distorting the local geometry of the molecules.[6,24] In any case, at least two types of emissive centers are present in the PPP-SO/PDDA mixture in 2-propanol (dual emission). It should be noted that PPP-SO/PDDA mixtures both in water and 2-propanol exhibited strong Tyndall scattering as shown in the inset in Fig. 2d, so they should have nano-architectures in the solutions.

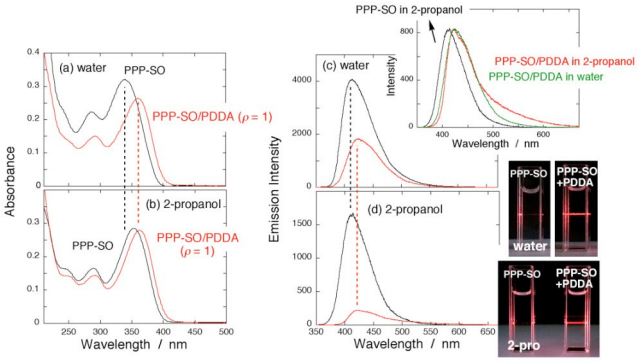

Fig. 2. (a) or (b) Absorption spectra of pristine PPP-SO (black curve) and PPP-SO/PDDA (ρ = 1, red curve) in water or 2-propanol, respectively. (c) or (d) Emission spectra of pristine PPP-SO (black curves) and PPP-SO/PDDA (ρ = 1, red curves) in water or 2-propanol, respectively. Fluorescence spectra are obtained upon excitation at 360 nm. Inset in (c) displays normalized emission spectra of PPP-SO in 2-propanol, PPP-SO/PDDA in water and that in 2-propanol. Inset in (d) shows Tyndall scattering images obtained by using He-Ne laser.

Morphology- and size-dependent emission properties: *Nanoparticles* versus *soft-agglomerates*

In our previous studies on organic nanoparticles of small ionic molecules, spectroscopic properties (and thereby particle sizes) have been frequently dependent on the charge stoichiometry (= ρ value). To examine whether this trend is observable in the present PPP-SO/PDDA systems, and whether polyelectrolyte nanoparticles are produced or not, we prepared a series of PPP-SO/PDDA systems in water and in 2-propanol as a function of ρ. Absorption, fluorescence, and excitation spectra of PPP-SO/PDDA mixtures in water or in 2-propanol are shown in Fig. 3. Fluorescence quantum yields (Φ_f) of these samples are summarized in Table 1. Basically, at any ρ value, absorption spectra of 2-propanolic PPP-SO/PDDA mixtures were similar to those in water, suggesting that both samples have similar conjugation-length segments or molecular conformations with each other. However, with a close inspection of these absorption spectra, the peak energy was slightly ρ-dependent for the 2-propanolic samples; that is, with an increase in ρ, the peak position was slightly red-shifted from ~362 nm (ρ = 1) to ~366 nm (ρ = 4), whereas no peak shift was detected for the PPP-SO/PDDA mixtures in water. This means that, in 2-propanol, the

conjugation length and/or degree of structural order of PPP-SO polymer backbones increases with an increase in the fraction of PDDA.

Emission spectra of PPP-SO/PDDA systems in 2-propanl were significantly different from those in water: (i) Fluorescence quenching is significant (for example, $\Phi_f = 0.04$ at $\rho = 1$, ~16% with respect to that of the aqueous sample). (ii) The green-site emission is prominent when the ρ value becomes large, yielding whitish-blue color emission as shown in the inset in Fig. 3d ($\rho = 4$). In other words, the emission spectra are strongly ρ-dependent for the 2-propanilic samples; with an increase in ρ, the green-site emission also increased. In sharp contrast, almost no ρ dependence was observed for the aqueous PPP-SO/PDDA mixtures. In addition, the fluorescence quantum yields showed little dependence on the ρ value.

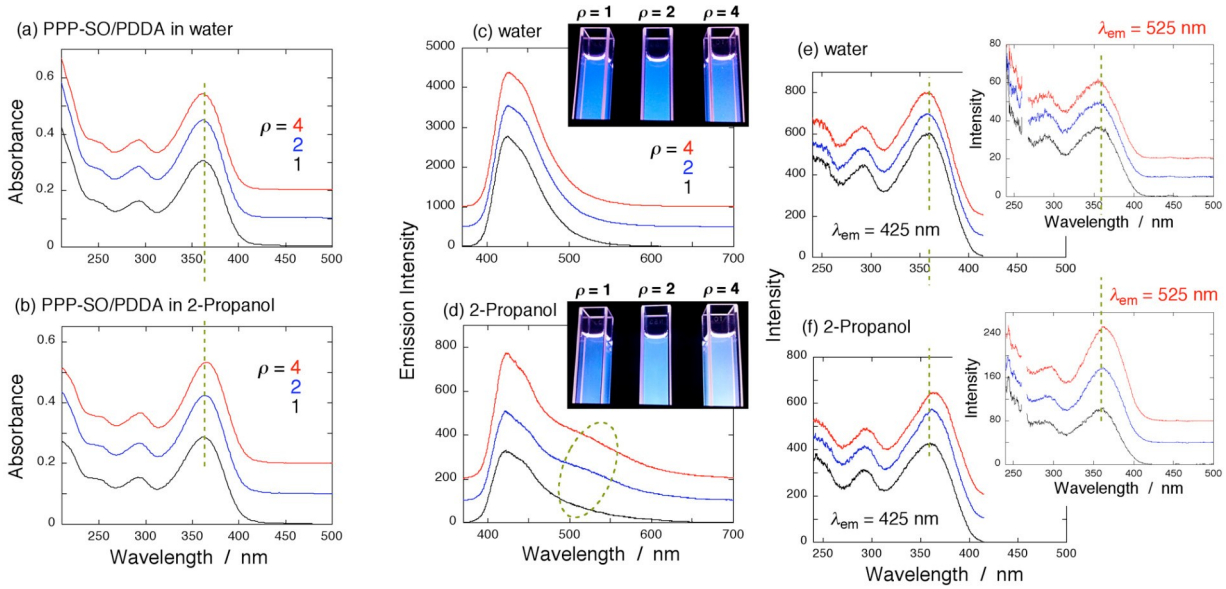

Fig. 3. (a) and (b) Absorption spectra of PPP-SO/PDDA mixtures in water and in 2-propanol as a function of ρ, respectively. The spectra are offset by a constant. (c) and (d) Fluorescence spectra of PPP-SO/PDDA mixtures in water and in 2-propanol as a function of ρ, respectively (λ_{ex} = 360 nm). The spectra are offset by a constant. Insets are photos of the fluorescence from the samples taken under 365 nm UV light irradiation. (e) and (f) Excitation spectra of PPP-SO/PDDA mixtures in water and in 2-propanol as a function of ρ, respectively. The emission is monitored at 425 (blue-site) or 525 nm (green-site). The spectra are offset by a constant.

The origin of emission can be derived from the excitation spectra, and comparison between the excitation and absorption spectra may give significant information on the blue-site/green-site emissive centers. The excitation spectra were monitored at λ_{em} = 425 nm or 525 nm for both series of samples (Figs. 3e and 3f for the aqueous and 2-propanolic samples, respectively). In PPP-SO/PDDA mixtures in water, the excitation peaks appeared at 358–359 nm (or 356–357 nm) when the emission was monitored at 425 nm (or 525 nm), respectively; the peak energies are ~30 meV higher than those for the π-π* absorption peaks (361–362 nm). Note that the aqueous PPP-SO/PDDA systems showed almost no green-site emission. This means that emission involved in conformational relaxation of the polymer backbone can be ruled out, because, if such relaxation occurs, the excitation peak positions should be at least identical with those of absorption. Hence it is reasonable to consider that the emission originates mainly from segments with relatively short conjugation length, and the observed discrepancy of the peaks between absorption and excitation spectra indicates that excitation energy of long(er) conjugation-length segments can be readily dissipated to some non-radiative bottle-necks. The H-type aggregates of π-conjugated backbones may contribute to the emission since an intensity of high-energy side (250–300 nm) of the excitation spectra monitored at 525 nm is stronger than that monitored at 425 nm. In this case, fluorescent H-type aggregates can be rationalized within the concept of exciton theory by considering a small transition probability caused by a slight rotation of the two-coupled chromophores;[9] however, the lack of hypsochromic absorption bands originated from H-aggregation (see Fig. 3a) suggests that its contribution is very small.

Table 1. Fluorescence quantum yields of various PPP-SO-based samples.

sample	solvent	charge ratio (ρ)	Φ_f
PPP-SO	water	-----	0.55
	2-propanol	-----	0.61
PPP-SO/PDDA	water	1	0.25
		2	0.26
		4	0.29
PPP-SO/PDDA	2-propanol	1	0.04
		2	0.054
		4	0.074

On the other hand, in PPP-SO/PDDA systems in 2-propanol, which had two distinct emissive centers in the samples, excitation spectra monitored at both 425 nm (blue-site) and 525 nm (green-site) are fairly ρ dependent. All these peaks were almost identical with those observed in the absorption spectra at any ρ value, and slightly shifted to red as a function of the ρ. These interesting facts suggest that the emission is originated from *single excitation species*, and the green-site emission should be due to (i) the result on the energy transfer to a trap-site with lower energy on the polymer backbone (including conformational relaxation), or excimer formation which likely involves π-π* stacking

interactions in the excited state between phenylene rings on adjacent chains stabilized by PDDA cations;[25] or (ii) long-conjugation segments in the polymer chain which can emit fluorescence at a low-energy region.[10] In any case, the origin of the observed emission significantly differs between the aqueous and 2-propanilic PPP-SO/PDDA systems.

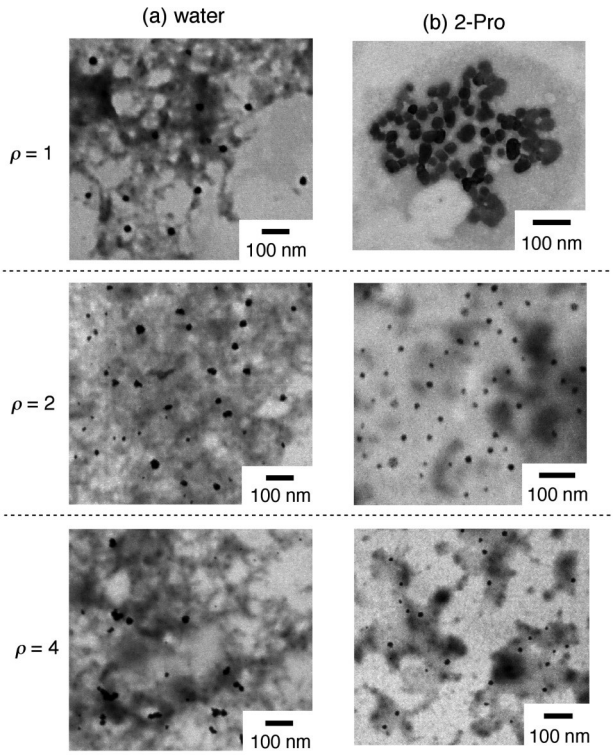

Fig. 4. (a) and (b) Typical STEM images for the PPP-SO/PDDA in water and in 2-propanol, respectively. The images are taken as a function of ρ.

As described before, polyion association between PPP-SO and PDDA in water and in 2-propanol brought about strong Tyndall scattering, hence to examine the relationship between their spectroscopic properties and morphologies, electron microscopy was conducted. Typical STEM images for the PPP-SO/PDDA (prepared at ρ = 1, 2, and 4) in water as well as those in 2-propanol are shown in Fig. 4. For the aqueous sample at ρ = 1, we found small particles with the diameter ranged in 20–30 nm, but widely-spread film-like features were dominant in the image. In addition, the STEM images (or morphology) did not change even when the ρ value increased, suggesting that nanoparticle formation is very partial (or incomplete) and thus the PPP-SO/PDDA polyion complex mostly exists in a *deformable soft-agglomerate* morphology. This observation is in good agreement with the spectroscopic data showing almost no ρ dependence. Note that, at ρ = 2 and 4, an excess PDDA would blur the images of the specimens. In contrast, well-defined polymer nanoparticles were successfully synthesized in 2-propanol by the *NAPA* approach. The STEM images reveal that roughly spherical nanoparticles have the diameter of 30–60 nm (ρ = 1), 20–30 nm (ρ = 2) or 10–30 nm (ρ = 4). In addition, at ρ = 1, nanoparticles tend to aggregate for prolonged periods; indeed, the dispersion prepared at ρ = 1 often produced some precipitates in about a week. Importantly, as the ρ increases, the particle size slightly decreases. It should be also emphasized that, in contrast to the π-conjugated polymer nanoparticle systems synthesized by the reprecipitation method,[8,26] which commonly yield blue-shifted absorption spectra as compared to those of the liberated polymer solution, the present ion-based nanoparticle system involves no shift in the absorption bands in comparison to that of the solution-phase polyion complexes, despite the behavior that compact globulization upon nanoparticle formation generally requires geometrical constraint that may bring about an overall decrease in the conjugation length attributable to the bending or kinking (disordering) of the polymer backbones.[22] The absence of further disordering upon nanoparticle formation from polyion complexes can be due to strong electrostatic attraction between PPP-SO and PDDA, and the interaction energy should be stronger than that for the folding of the rigid polymer backbone. In a sense, PDDA polycations would protect the rigid π-conjugated polymer scaffolds.

At the end of this section, we discuss the difference in the fluorescence intensity of PPP-SO/PDDA system in water and in 2-propanol. From Table 1, fluorescence quantum yield (Φ_f) of the soft-agglomerates was overall higher than that of the polymer nanoparticles. This is not due to the solvent effect because, in the absence of PDDA, Φ_f obtained in aqueous solution was almost identical with that in 2-propanol. Hence their morphological difference (and consequent interchromophore interaction) is responsible for this behavior. The *solid-state* PPP nanoparticles are substantially composed of densely-packed π-conjugated polymers, so the interchain quenching should be the major origin for the relatively low Φ_f values in the 2-propanilic PPP-SO/PDDA system.

Fluorescence anisotropy

Fluorescence anisotropy (FA) or depolarization is a direct measure of the angular correlation between the absorption and the emission transition dipoles.[27] In general, if molecular rotation and/or energy migration (transfer) of fluorophores does not occur within the excited-state lifetime, the emission is not depolarized and thus the anisotropy does not change; it is known that upper and lower bounds for the anisotropy are 0.4 (collinear absorption and emission transitions) and –0.2 (orthogonal absorption and emission transitions).[27] To further examine the origin of the emission from "*nanoparticles*" or "*soft-agglomerates*", the FA was measured. Figs. 5b and 5c show wavelength-dependent fluorescence anisotropy for the PPP-SO/PDDA-based soft-agglomerates in water and that for the nanoparticles in 2-propanol, respectively, together with that for the pristine PPP-SO dissolved in water and 2-propanol (control experiments; Fig. 5a). The excitation wavelength is 360 nm, which induces a transition polarized in the long-axis (main-chain) of the polymer.[16]

In polyelectrolyte solutions (both in water and in 2-propanol, Fig. 5a), pristine PPP-SO has a nonzero fluorescence anisotropy of about 0.3 (high FA value), so the rotation of polymer backbone is very slow even in the fluids. This also means that large conformational relaxation such as stretching (or bending) of polymer chains is unlikely to occur within the emission lifetime (~1 ns),[16] since such relaxation would cause the disruption of the conjugation along with a deviation in dipole orientation and accordingly reduce the anisotropy. For the *soft-agglomerates* in water (Fig. 5b), a loss of fluorescence anisotropy was trivial (FA

= ~0.3) at all emission wavelengths for any ρ value, suggesting that the rotation of phenylene backbone is still slow. On this basis, it is reasonable to conclude that emission from the PPP-SO/PDDA soft-agglomerates in water essentially stems from relatively short conjugation-length segments under direct excitation (and then *not* from the H-aggregates).

In contrast, for the PPP nanoparticles produced in 2-propanol (Fig. 5c), we found that (i) fluorescence anisotropy was almost constant (~0.3) at $\lambda_{em} \leq$ ~470 nm (blue-site) for all nanoparticle samples; (ii) at ρ = 1, the loss of fluorescence anisotropy was particularly significant at $\lambda_{em} \geq$ ~470 nm (green-site); (iii) at ρ = 2 and 4, the decrease in the anisotropy was very small at $\lambda_{em} \geq$ ~470 nm. It is known that the excitonic properties of conjugated polymers allow an excitation to move along the chain from one chromophore site to another of lower energy (= *trap-site*), bringing about a bathochromic shift in the emission.[24] The orientation of the dipole is determined by the chromophore's position along the chain, so the exciton migration will reorient the dipole from its initial orientation and reduce the measured fluorescence anisotropy. Therefore, the main origin of the green-site emission from the large PPP nanoparticles (prepared at ρ = 1) can be either excitation migration (and subsequent non-radiative energy transfer) to a certain emissive trap-site on the polymer backbone, or formation of excimer-like states between fluorophores (but in a later section, we will describe that excimer formation is a less likely origin for the green-site emission from a viewpoint of molecular geometries). Here, the "trap-site" is probably low-energy structural defects including conformational distortions (relaxation) arising from the polyion interactions, modulation in the backbone polymer propagation, and/or inhomogeneities due to neighboring chromophore aggregation.[28]

It is quite natural that such excitation migration (and subsequent energy transfer) will also occur in smaller nanoparticles prepared at ρ = 2 and 4, but interestingly, considering a smaller loss of fluorescence anisotropy in the green-site emission as compared to those obtained at ρ = 1 as well as the ρ-dependent peak red-shift observed in the excitation spectra (λ_{em} = 525 nm), the exclusive excitation of the chromophoric segments having a long effective conjugation length greatly (and additionally) contributes to the green-site emission. Hence the size-dependent enhancement in the green-site emission for the PPP nanoparticles can be due to an increase in the long conjugation-length segments under direct excitation.

One may say that the PDDA polycations can induce chain-chain interactions in or between PPP-SO polyelectrolyte(s) through electrostatic attraction in the PPP nanoparticle, and thus induce "certain disorders" in the nanoparticle.[29,30] Meanwhile, it is reasonable to consider that the environment of outermost PPP-SO fluorophore units on the nanoparticle surface is manifestly different from that inside the nanoparticle; in other words, approximately half of the bonds for the interfacial PPP-SO differs from those for the inner PPP-SO (including homomolecular and heteromolecular interactions). According to the present results, the interfacial region of nanoparticles would contribute to an increase in stabilizing the long conjugation-length segments of the polymer. From a viewpoint of surface chemistry, a small (large) solid-state particle has a large (small) surface-to-volume ratio, respectively, so small PPP nanoparticles can have an increased number of segments with relatively long conjugation length, exhibiting enhanced green-site emission. As for the "trap-site" or "low-energy defect", on the other hand, its location (whether it is on the nanoparticle surface or inside the particle) is not clear at present, but they can be mostly located inside the nanoparticles in consideration with the size-dependent FA value of PPP nanoparticle samples and the emission properties of bulk films that will be discussed in the next section.

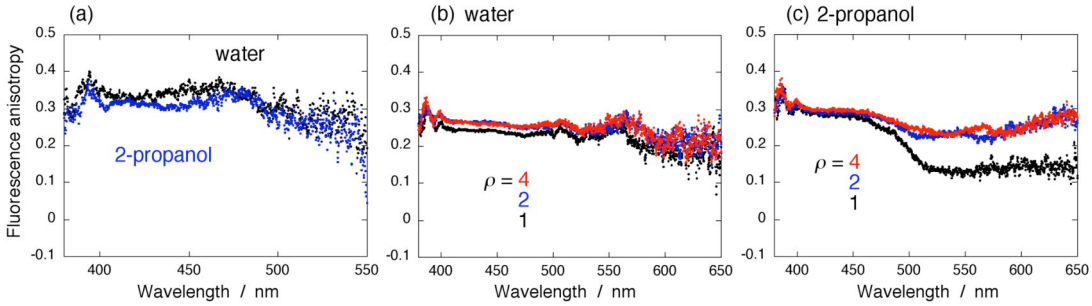

Fig. 5. (a) Wavelength-dependent fluorescence anisotropy (FA) for pristine PPP-SO dissolved in water (black curve) and 2-propanol (blue curve). (b) and (c) Wavelength-dependent FA for the PPP-SO/PDDA deformable agglomerates in water and those for nanoparticles in 2-propanol, respectively. Black, blue, and red curves correspond to the data obtained at ρ = 1, 2, and 4, respectively.

Bulk films

In the PPP nanoparticles, the green-site emission was strongly associated with the outermost surface (interface) region of the solid-state nanoparticle. This indiates that, if a bulk solid film is prepared from aqueous PPP-SO/PDDA soft-agglomerates, (i) stronger green-site emission will be expected compared to that from the soft-agglomerates because the film production process can convert the soft-species into a hard matter; (ii) weaker green-site emission will be expected compared to that from PPP nanoparticles dispersed in 2-propanol because the solid film has less outermost surface area than the nanoparticles. Then the absorption and fluorescence spectra of PPP-SO/PDDA or pure PPP-SO films, which were prepared by a drop cast of the corresponding solution, were compared to those of various samples. Here ρ is unity. The spectroscopic data are shown in Figs. 6a and 6b. For clarity, comparison of the peak positions for various PPP-SO-related samples is schematically displayed in Fig. 6c. The absorption peak was red-shifted from 339 to 362 nm when the pristine PPP-SO aqueous solution was converted to the corresponding thin solid film, suggesting that the effective

conjugation length is longer for the solid film than that dissolved in water. On the other hand, irrespective of the morphology of PPP-SO/PDDA complexes (soft-agglomerates, nanoparticles, or solid films), their absorption peak positions were essentially unchanged. This means that absorption properties of the PPP chromophores are solely governed by electrostatic interactions with PDDA, and it definitely extends the effective conjugation length of PPP-SO backbones probably through the planarization of phenylene chains. The striking behavior lies in their emission properties (Fig. 6b), that is, they are strongly *morphology dependent*. Although quenching in the blue-site emission was more or less present in the solid-state nanoparticles and thin films, the nanoparticle species had the strongest green-site emission, whereas the soft-agglomerates exhibited the weakest. As expected, the film had the intermediate character for the green-site emission,‡ in good agreement with the observation that the smaller the particle size is, the stronger the green-site emission intensity is. Conclusively, π-conjugated polymer PPP nanoparticles synthesized via the NAPA approach can tune the emission properties by controlling their morphology including the size of the nanoparticles.

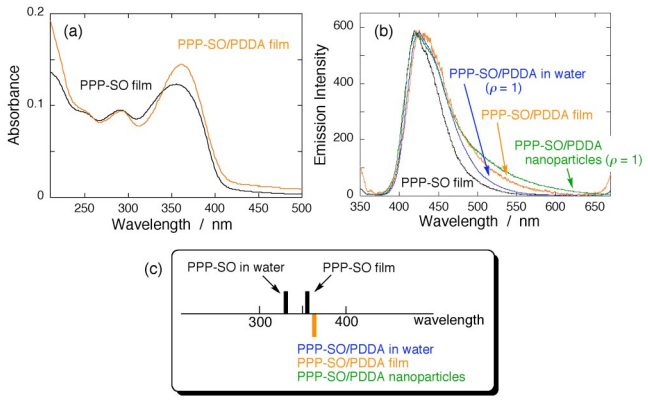

Fig. 6. (a) Absorption and (b) emission spectra of PPP-SO and PPP-SO/PDDA thin films on a quartz substrate. For preparing the PPP-SO/PDDA film, solutions with $\rho = 1$ was used. Emission spectra of PPP-SO/PDDA soft-agglomerates and nanoparticles ($\rho = 1$) are also shown for comparison. (c) Comparison of absorption maxima for various samples.

Geometry computations

As mentioned before, we have reached that the main origin of the green-site emission from PPP nanoparticle samples (particularly the case of $\rho = 1$) could be either the energy transfer to a trap-site (or low-energy defect) on the polymer backbone or formation of excimer-like states between the fluorophores. To investigate how the countercations in the vicinity of the anionic PPP-SO influence its polymer backbone geometry, and to clarify whether the excimer formation between phenylene units is possible or not, we conducted calculations on simple structural models of ion-pair adducts of PPP-SO and PDDA analogues. For a model unit of PPP-SO, four phenylene rings having four propanesulfonate substituents per chain are considered (see Fig. 7a). In the case of a PDDA model, we chose a substituted 1,1-dimethylpyrrolidinium cation that corresponds to the monomer unit of PDDA (see Fig. 7b), and placed eight pyrrolidinium cations in the vicinity of the sulfonate groups of the model PPP-SO unit to be charge neutral (= 2•(PPP-SO)–8•PDDA). We optimized the ground-state geometry of the structure with the Gaussian 09 program at the semi-empirical PM6 level.[9c,17] Fig. 7c or 7d displays a typical optimized structure of 2•(PPP-SO)–8•PDDA or sole PPP-SO units extracted from Fig. 7c, respectively. Note that, for clarity, terminal sulfonate substituents are replaced by hydrogen atoms in Fig. 7d. Our simple models can be a good indication for evaluating the excimer formation of PPP-SO in the presence of PDDA species.

An excimer is a complex (or excited dimer) between an aromatic molecule in the excited state and the same species in the ground state. It is well known that the formation of excimers of aromatics is restricted to parallel, cofacial configuration with an interplanar distance of 3–4 Å.[31] In the present case, a large conformational change of phenylenes along the polymer backbone is more or less required.[32] According to Fig. 7d, interchain phenylene rings are separated at least 5~6 Å and thus are hard to form excimers with cofacial configuration of two aromatic moieties by their simple conformational change. Hence we can conclude that the excimer formation is unlikely.

Additionally, we found that, in the presence of PDDA cations, conformations of PPP-SO (phenylene unites) are obviously different from those in the absence of PDDA as shown in Figs. 7a and 7d. For example, in Fig. 7a or 7d, the dihedral angle measured for the four phenylene sequences in the PPP-SO model is ranged in 32–50° or 32–88°, respectively, resulting in a high possibility of backbone structures having azimuthal kinks and/or torsions (leading to certain defects).[33] Although the present model only gives a possibility to produce local distortions in (on) the polymer backbone, we can deduce that the origin of the green-site emission from PPP nanoparticle samples (particularly at $\rho = 1$) should be non-radiative energy transfer to a low-energy defect (trap-site) on the polymer backbones. We believe successful synthesis of such π-conjugated polyelectrolyte nanoparticles in desired emission properties will make these materials highly attractive for applications in various areas such as optoelectronics and bioimaging in the future.

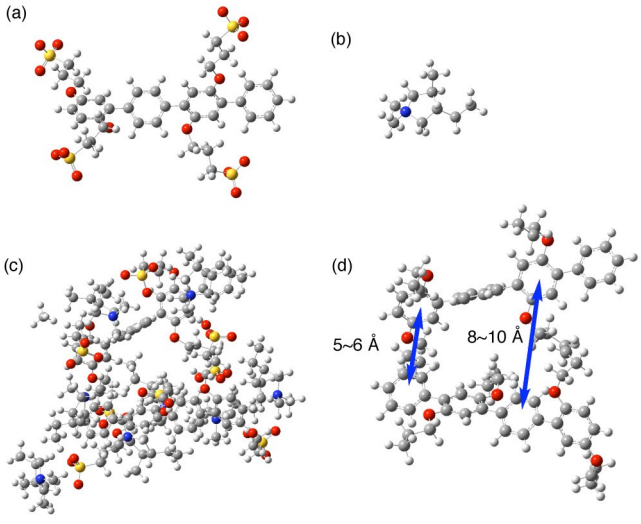

Fig. 7. (a) and (b) Optimized structures of a model of PPP-SO and that of PDDA, respectively. (c) Optimized structure of an adduct of 2•(PPP-SO)–8•PDDA model. (d) Sole PPP-SO geometry extracted from the complex shown in (c). All calculations were conducted at the semi-empirical PM6 level.

Conclusions

In summary, a facile method was developed to synthesize fluorescent π-conjugated polymer (polyelectrolyte) nanoparticles of poly(*p*-phenylene) anionic derivative PPP-SO; poly(2,5-bis(3-sulfonatopropoxy)-1,4-phenylene-*alt*-1,4-phenylene). It was based on *n*ano-*a*gglomeration via *p*olyion *a*ssociation (*NAPA* approach) that includes polyion complex formation between PPP-SO and poly(diallyldimethylammonium) (PDDA) cation, and subsequent globulization to fabricate nanoarchitectures in 2-propanol (= poor solvent for the PPP-SO/PDDA polyion complex). The particle size could be tuned by the net charge ratio between the PPP-SO and PDDA. A striking feature was a dual emission property; the green-site emission (≥ ~500 nm) became more intense when the size of the nanoparticles decreased. On the basis of fluorescence anisotropy measurements, this green-site emission can be due either to the non-radiative excitation energy transfer to an emissive trap-site or low-energy defect on the polymer backbone or exclusive excitation of the chromophoric segments having a long effective conjugation length, where the latter mechanism was significant in a small particle size region. Such nano-engineering methodology for functional polymers or polyelectrolytes will play a fundamental role in an entire new class of fluorescent organic nanomaterials with dimension dependence.

Acknowledgements

The present work was in part supported by Grant-in-Aids for Scientific Research (C: 15K04593 (H. Y.)) from Japan Society for the Promotion of Science (JSPS).

Notes and references

§ In general, it is known that molecular weights (M_w) of water-soluble conjugated polymers are difficult to determine using standard GPC methods due to the high affinity of the polymer for many gel or column matrices, their aggregation behavior and rigid nature.[16] Hence in *ref.* 16, facile *minimum* M_w estimation of water-soluble PPP (PPP-SO) based on absorption spectroscopy has been proposed. Meanwhile, we tried to estimate the number of repeat units (N) in PPP-SO by measuring dynamic light scattering (DLS). Assuming a random walk conformation, the hydrodynamic diameter (D_H) of the polymer is roughly estimated as ($a \times \sqrt{N}$), where a is the length of the repeat unit (= 1.2 nm).[34] From the DLS data (0.01 wt% PPP-SO solution), the mean D_H value of pristine PPP-SO was ~9 μm, so N is 5.6×10^7, implying the molecular weight of ~2×10^{10}. Such a large M_w value suggests that the PPP-SO polyelectrolytes would be aggregated.[35]

‡ Emission spectrum of the PPP-SO/PDDA film prepared by a drop cast of the corresponding 2-propanol solution is also shown in the ESI†, exhibiting an almost identical spectral shape with that prepared by the corresponding aqueous solution.

1 J. H. Burroughes, D. D. C. Bradley, A. R. Brown, R. N. Marks, K. Mackay, R. H. Friend, P. L. Burns and A. B. Holmes, *Nature*, 1990, **347**, 539.
2. J. C. Bolinger, M. C. Traub, J. Brazard, T. Adachi, P. F. Barbara and D. A. Vanden Bout, *Acc. Chem. Res*., 2012, **45**, 1992.
3. D. Tuncel and H. V. Demir, *Nanoscale*, 2010, **2**, 484.
4. D. T. McQuade, A. E. Pullen and T. M. Swager, *Chem. Rev*., 2000, **100**, 2537.
5. X. L. Feng, L. B. Liu, S.Wang and D. B. Zhu, *Chem. Soc. Rev*., 2010, **39**, 2411.
6. K. Landfester, *Angew. Chem., Int. Ed*., 2009, **48**, 4488.
7. P. Sarrazin, D. Chaussy, L. Vurth, O. Stephan and D. Beneventi, *Langmuir*, 2009, **25**, 6745.
8. C. Wu, C. Szymanski and J. McNeill, *Langmuir*, 2006, **22**, 2956.
9. (a) H. Yao and T. Enseki, *J. Photochem. Photobiol. A: Chem*., 2013, **271**, 124; (b) H. Yao and T. Funada, *Chem. Commun*., 2014, **50**, 2748; (c) H. Yao and K. Ashiba, *RSC Advances*, 2011, **1**, 834.
10. C. Fukui and H. Yao, *J. Mater. Res*., 2015, **30**, 10.
11. (a) X. Wang, L. C. Groff and J. D. McNeill, *Langmuir* 2013, **29**, 13925; (b) F. W. D. Rost, *Fluorescence Microscopy*, Cambridge University Press, Cambridge, UK, 1992, Vol. 1.
12. (a) M. Banerjee, R. Shukla and R. Rathore, *J. Am. Chem. Soc*., 2009, **131**, 1780; (b) L. W. Shacklette, H. Eckhardt, R. R. Chance, G. G. Miller, D. M. Ivory and R. H. Baughman, *J. Chem. Phys*. 1980, **73**, 4098.
13. (a) F. Meghdadi, S. Tasch, B. Winkler, W. Fischer, F. Stelzer and G. Leising, *Synth. Met*., 1997, **85**, 1441; (b) J. W. Baur, S. Kim, P. B. Balanda, J. R. Reynolds and M. F. Rubner, *Adv. Mater*., 1998, **10**, 1452.
14. (a) D. M. Gale, *J. Appl. Polym. Sci*., 1978, **22**, 1971; (b) K. N. Baker, A. V. Fratini, T. Resch, H. C. Knachel, W. W. Adams, E. P. Socci and B. L. Farmer, *Polymer*, 1993, **34**, 1571.
15. J.-L. Bredas, D. Beljonne, V. Coropceanu and J. Cornil, *Chem. Rev*., 2004, **104**, 4971.
16. S. Kim, J. Jackiw, E. Robinson, K. S. Schanze, J. R. Reynolds, J. Baur, M. F. Rubner and D. Boils, *Macromolecules*, 1998, **31**, 964.
17. M. J. Frisch, G. W. Trucks, H. B. Schlegel, G. E. Scuseria, M. A. Robb, J. R. Cheeseman, G. Scalmani, V. Barone, B. Mennucci, G. A. Petersson, H. Nakatsuji, M. Caricato, X. Li, H. P. Hratchian, A. F. Izmaylov, J. Bloino, G. Zheng, J. L. Sonnenberg, M. Hada, M. Ehara, K. Toyota, R. Fukuda, J. Hasegawa, M. Ishida, T. Nakajima, Y. Honda, O. Kitao, H. Nakai, T. Vreven, J. A. Montgomery, Jr., J. E. Peralta, F. Ogliaro, M. Bearpark, J. J. Heyd, E. Brothers, K. N. Kudin, V. N. Staroverov, T. Keith, R. Kobayashi, J. Normand, K. Raghavachari, A. Rendell, J. C. Burant, S. S. Iyengar, J. Tomasi, M. Cossi, N. Rega, J. M. Millam, M. Klene, J. E. Knox, J. B. Cross, V. Bakken, C. Adamo, J. Jaramillo, R. Gomperts, R. E. Stratmann, O. Yazyev, A. J. Austin, R. Cammi, C. Pomelli, J. W. Ochterski, R. L. Martin, K. Morokuma, V. G. Zakrzewski, G. A. Voth, P. Salvador, J. J. Dannenberg, S. Dapprich, A. D. Daniels, O. Farkas, J. B. Foresman, J. V. Ortiz, J. Cioslowski, D. J. Fox, *Gaussian 09*, Gaussian, Inc., Wallingford CT, 2010.
18. W. J. MacKnight, E. A. Ponomarenko and D. A. Tirrell, *Acc. Chem. Res*., 1998, **31**, 781.
19. A. V. Kabanov, T. K. Bronich, V. A. Kabanov, K. Yu and A. Eisenberg, *J. Am. Chem. Soc*., 1998, **120**, 9941.
20. P. S. Kuhn, Y. Levin and M. C. Barbosa, *Chem. Phys. Lett*., 1998, **298**, 51.
21. P. B. Balanda, M. B. Ramey and J. R. Reynolds, *Macromolecules*, 1999, **32**, 3970.
22. G. Padmanaban and S. Ramakrishnan, *J. Am. Chem. Soc*., 2000, **122**, 2244.
23. G. A. Montano, A. M. Dattelbaum, H.-L. Wang and A. P. Shreve, *Chem. Commun*., 2004, 2490.
24. H. L. Vaughan, F. M. B. Dias and A. P. Monkman, *J. Chem. Phys*., 2005, **122**, 014902.
25. Gordon, M., Ware, W. R., Eds. *The Exciplex*; Academic Press: New York, 1975.
26. C. Szymanski, C. Wu, J. Hooper, M. A. Salazar, A. Perdomo, A. Dukes and J. McNeill, *J. Phys. Chem. B*, 2005, **109**, 8543.
27. M. N. Berberan-Santos and B. Valeur, *J. Chem. Soc. Faraday Trans*., 1994, **90**, 2623.
28. (a) A. Kadashchuk, A. Andreev, H. Sitter, N. S. Sariciftci, Y. Skryshevski, Y. Piryatinski, I. Blonsky and D. Meissner, *Adv. Func. Mater*., 2004, **14**, 970; (b) K. F. Wong, M. S. Skaf, C.-Y. Yang, P. J. Rossky, B. Bagchi, D. Hu, J. Yu and P. F. Barbara, *J. Phys. Chem. B* 2001, **105**, 6103-6107
29. Y.-H. Lin, C. Jiang, J. Xu, Z. Lin and V. V. Tsukruk, *Soft Matter*, 2007, **3**, 432.

30. J. Tang, W. J. Li, Y. Wang, B. Wang, J. Sun and B. Yang, *J. Photochem. Photobiol. A: Chem.*, 2001, **141**, 179.
31. (a) J. B. Birks, *Photophysics of Aromatic Molecules*, London, UK: John Wiley & Sons; 1970; (b) J. M. Robertson and J. G. White, *J. Chem. Soc*., 1947, 358.
32. Y. F. Huang, Y. J. Shiu, J. H. Hsu, S. H. Lin, A. C. Su, K. Y. Peng, S. A. Chen and W. S. Fann, *J. Phys. Chem. C*, 2007, **111**, 5533.
33. W. J. D. Beenken and T. Pullerits, *J. Phys. Chem. B*, 2004, **108**, 6164.
34. J. Wang, D. Wang, E. K. Miller, D. Moses, G. C. Bazan and A. J. Heeger, *Macromolecules,* 2000, **33**, 5153.
35. P. Kaur, H. Yue, M. Wu, M. Liu, J. Treece, D. H. Waldeck, C. Xue and H. Liu, *J. Phys. Chem. B*, 2007, **111**, 8589.

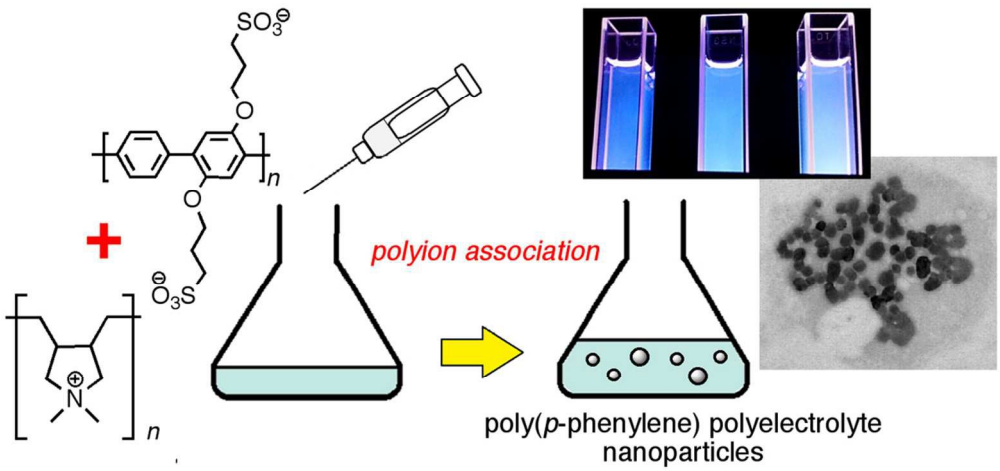

101x47mm (300 x 300 DPI)